This article was downloaded by: [University Of Gujrat]
On: 11 December 2014, At: 13:58
Publisher: Taylor & Francis
Informa Ltd Registered in England and Wales Registered Number: 1072954 Registered office: Mortimer House, 37-41 Mortimer Street, London W1T 3JH, UK

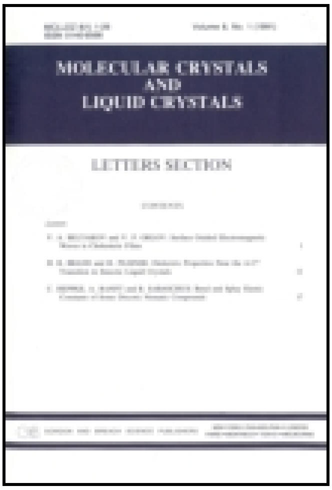

Molecular Crystals and Liquid Crystals
Publication details, including instructions for authors and subscription information:
http://www.tandfonline.com/loi/gmcl20

Enhancement Mechanisms of the Power Conversion Efficiency for the P3HT:PCBM Bulk Heterojunction Solar Cells with a LiF Cathode Buffer Layer Due to Thermal Annealing

Qifeng Han[ab], Narayanasamy Sabari Arul[a] & Tae Whan Kim[a]
[a] Department of Electronics and Computer Engineering, Hanyang University, 222 Wangsimni-ro, Seongdong-gu, Seoul 133-791, Korea
[b] Permanent address: Key Laboratory of Optoelectronics Materials and Devices, Shanghai Normal University, Shanghai, P. R. China

Published online: 06 Dec 2014.

To cite this article: Qifeng Han, Narayanasamy Sabari Arul & Tae Whan Kim (2014) Enhancement Mechanisms of the Power Conversion Efficiency for the P3HT:PCBM Bulk Heterojunction Solar Cells with a LiF Cathode Buffer Layer Due to Thermal Annealing, Molecular Crystals and Liquid Crystals, 602:1, 159-167, DOI: 10.1080/15421406.2014.944756

To link to this article: http://dx.doi.org/10.1080/15421406.2014.944756

PLEASE SCROLL DOWN FOR ARTICLE

Taylor & Francis makes every effort to ensure the accuracy of all the information (the "Content") contained in the publications on our platform. However, Taylor & Francis, our agents, and our licensors make no representations or warranties whatsoever as to the accuracy, completeness, or suitability for any purpose of the Content. Any opinions and views expressed in this publication are the opinions and views of the authors, and are not the views of or endorsed by Taylor & Francis. The accuracy of the Content should not be relied upon and should be independently verified with primary sources of information. Taylor and Francis shall not be liable for any losses, actions, claims, proceedings, demands, costs, expenses, damages, and other liabilities whatsoever or howsoever caused arising directly or indirectly in connection with, in relation to or arising out of the use of the Content.

This article may be used for research, teaching, and private study purposes. Any substantial or systematic reproduction, redistribution, reselling, loan, sub-licensing, systematic supply, or distribution in any form to anyone is expressly forbidden. Terms &

Mol. Cryst. Liq. Cryst., Vol. 602: pp. 159–167, 2014

ISSN: 1542-1406 print/1563-5287 online
DOI: 10.1080/15421406.2014.944756

Enhancement Mechanisms of the Power Conversion Efficiency for the P3HT:PCBM Bulk Heterojunction Solar Cells with a LiF Cathode Buffer Layer Due to Thermal Annealing

QIFENG HAN,[a] NARAYANASAMY SABARI ARUL,
AND TAE WHAN KIM*

Department of Electronics and Computer Engineering, Hanyang University,
Seongdong-gu, Seoul, Korea

The effect of thermal annealing on the device characteristics of the bulk heterojunction poly(3-hexylthiophene) (P3HT):fullerene derivative [6,6]-phenyl-C61-butyric acid methyl ester (PCBM) solar cells was investigated. Absorption spectra showed that the absorption intensity was highest for the P3HT:PCBM layer with a LiF layer annealed for 5 min. Atomic force microscopy images showed that the P3HT:PCBM layer with a LiF layer annealed for 5 min had the uniform surface morphology. The fabricated organic photovoltaic (OPV) cells annealed for 5 min showed the enhanced power conversion efficiency of 3.87% than that of the OPV cells annealed for 3 or 10 min.

Keywords Photovoltaic cells; P3HT:PCBM layer; power conversion efficiency; LiF cathode buffer layer; thermal annealing

Introduction

Organic photovoltaic (OPV) cells have currently been receiving considerable attention due to the gradual exhaustion of traditional fossil fuels [1–4]. OPV cells have emerged as excellent candidates due to their low cost, high-mechanical flexibility, light weight, high softness, and large absorption [5–8]. OPV cells with a bulk heterojunction (BHJ) structure have achieved power conversion efficiency (PCE) up to 10% under a standard solar spectrum, AM 1.5 G [9]. The prospect of potential applications of OPV cells utilizing organic layers has led to substantial research and development efforts to enhance the PCE of the OPV cells. A buffer layer has been introduced between the organic molecules and the metal cathode in the OPV cells to improve their PCE [10]. A LiF layer, acting as a cathode buffer layer, increases the open-circuit voltage (Voc) of OPV cells [11]. Some studies on the enhancement of the device performance in OPV cells have been performed by using

---

*Address correspondence to Prof. Tae Whan Kim, Department of Electronics and Computer Engineering, Hanyang University, 222 Wangsimni-ro, Seongdong-gu, Seoul 133-791, Korea (ROK). Email: twk@hanyang.ac.kr

[a] Permanent address: Key Laboratory of Optoelectronics Materials and Devices, Shanghai Normal University, Shanghai, P. R. China

Color versions of one or more of the figures in the article can be found online at www.tandfonline.com/gmcl.

thermal annealing treatment [12, 13]. Even though some studies concerning increases in the shunt resistance, the built-in potential, and the PCE of OPV cells fabricated utilizing poly (3-hexylthiophene) (P3HT):fullerene derivative [6, 6]-phenyl-C61-butyric acid methyl ester (PCBM) BHJs due to thermal annealing have been reported [14, 15], the effect of thermal annealing time on the PCEs of heterojunction OPV cells made of P3HT:PCBM BHJs and dependent on thermal annealing time have not clearly clarified yet. Furthermore, studies on the enhancement mechanisms of the PCE for OPV cells based on the hybrid organic layer due to thermal annealing are necessary to enhance the device efficiency.

This paper reports data for the effect of thermal annealing time on the PCEs of P3HT:PCBM BHJ solar cells with a LiF cathode buffer layer. Absorption measurements were performed to investigate the intensities and the positions of the absorption peaks, and atomic force microscopy (AFM) measurements were carried out to investigate the surface properties of the P3HT:PCBM nanocomposites with a LiF layer. X-ray photoelectron spectroscopy (XPS) measurements were performed to investigate the structural properties of the layers. Current density-voltage (J-V) measurements were performed to investigate the possibility of fabricating OPV devices based on P3HT:PCBM nanocomposites. The PCE enhancement mechanisms of OPV cells due to thermal treatment were described on the basis of the experimental results.

Experimental

Device Preparation

The OPV cells fabricated in this study were prepared on indium-tin-oxide (ITO)-coated glass substrates, and the sheet resistance of the ITO thin film was approximately 10 Ω/sq. The ITO substrates were cleaned in acetone and isopropanol by using an ultrasonic cleaner with a sonication amplitude of 135 W and a frequency of 42 kHz for 10 min. After the chemically cleaned ITO-coated glass substrates had been treated with an ultraviolet-ozone cleaner, poly (3,4-ethylenedioxythiophene):poly (styrenesulfonate) (PEDOT:PSS) was spin-coated onto the ITO-coated glass substrates at 4500 rpm for 40 s in a glove box under a high-purity N_2 atmosphere. The active layer consisting of the P3HT:PCBM solution (20-mg/ml P3HT and 16-mg/ml PCBM) prepared in 1,2-dichlorobenzene was spin-coated on PEDOT:PSS anode buffer layers at 1500 rpm for 60 s. Subsequently, the LiF cathode buffer layers were deposited on the active layers by using thermal evaporation; then, an Al layer with a thickness of 100 nm was formed. The active area of the fabricated cell was 2 mm × 2 mm. Finally, the fabricated OPV cells were annealed for 3, 5, or 10 min at 140°C on a hot plate [16–18]. Figure 1 shows a schematic diagram of the fabricated OPV cells consisting of a cathode buffer layer, Al/LiF/P3HT:PCBM/PEDOT:PSS/ITO structure.

Characterization Methods

The optical absorption spectra were measured by using an SHIMADZU UV-2401PC spectrophotometer. The AFM measurements were performed by using an XE-100 atomic force microscope. XPS spectra were measured by using an ESCALAB spectrometer with an excitation source. The evolutions of surface morphology were studied by using AFM, and XPS with an Al Kα radiation source was used to determine the chemical bonding. The current density-voltage (J-V) curves were measured by using a Keithley 2400 source meter in the dark and under illumination. The photovoltaic characteristics were measured under AM 1.5 simulated illumination with an intensity of 100 mW/cm^2.

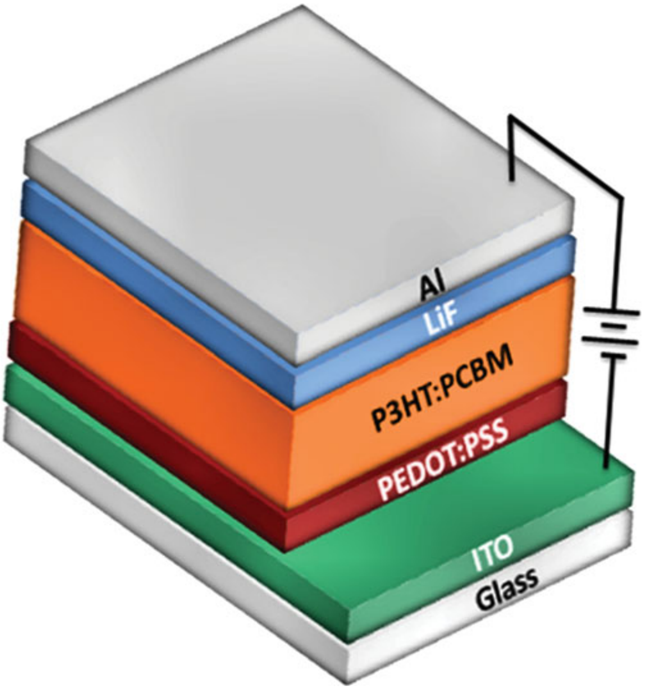

Figure 1. Schematic diagram of the fabricated organic photovoltaic cells consisting of a cathode buffer layer, Al/LiF/P3HT:PCBM/PEDOT:PSS/ITO structure.

Results and Discussion

Absorption Spectra

The absorption spectra of the P3HT:PCBM active layer with a 1-nm-thick LiF layer annealed for 3, 5, or 10 min at 140°C were shown in Fig. 2. The thicknesses of the P3HT:PCBM layers are not significantly changed due to the variations of the annealing temperatures. While P3HT molecules in the P3HT:PCBM layer typically contributed to absorb in a long wavelength region, the pristine PCBM molecules absorbed a short wavelength light [19].

The P3HT:PCBM active layer with a LiF layer annealed for 5 min showed the strongest absorption intensity among all devices. While the absorption intensity of the P3HT:PCBM thin film annealed for 10 min in the P3HT absorption region was similar to that of the film annealed for 3 min, the absorption intensity corresponding to the PCBM region was low. Because an absorption band was the characteristic peak due to the π-π^* transition of the P3HT molecules, the enhanced intensity of the sample annealed 5 min was attributed that the π-π stacking of P3HT molecules was increased in the P3HT:PCBM layer.

In addition, the improved absorption intensities for the P3HT:PCBM layers annealed for 5 min, in comparison with that for the layer annealed for 3 min, are attributed to an increase in the light reflection between the P3HT:PCBM active layer and the LiF heterointerface due to tight contact formation [20]. After 10 min annealing, the PCBM absorption intensity dramatically decreased. The surface of the PCBM for the P3HT:PCBM layer annealed at 10 min was not as uniform as that for the P3HT:PCBM layer annealed at 5 min, and was not significantly affected by the LiF layer.

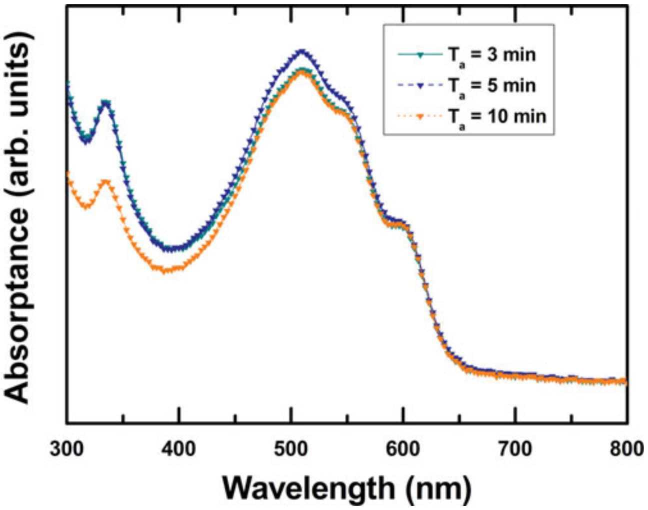

Figure 2. Normalized absorption spectra of the active P3HT:PCBM layers with a LiF layer and annealed for 3, 5, or 10 min at 140°C.

Surface Topology and Composition Analysis

AFM images of the P3HT:PCBM layer with a LiF layer annealed for 3, 5, or 10 min at 140°C are shown in Fig. 3. The surface of the P3HT:PCBM layer with a LiF layer annealed for 5 min was smoother than that of the P3HT:PCBM layer with a LiF layer annealed for 3 or 5 min. The rough surface of the P3HT:PCBM annealed for 10 min was caused by bulges on the surface of the layer resulting from an aggregation of the PCBM, leading to the low absorption in the PCBM absorbing region [21]. The flat and uniform surface of the P3HT:PCBM layer produced a high-quality heterointerface between the LiF layer annealed for 5 min and the Al cathode, resulting in an effective decrease in the charge-transport distance and the contact resistance [22].

Figure 4 shows XPS spectra of the P3HT:PCBM layers with a LiF layer annealed for 3, 5, or 10 min at 140°C. While the P3HT molecules contained sulfur without oxygen, the PCBM molecules contained oxygen without sulfur. The S 2p and O 1s photoelectron peaks corresponded to the P3HT and the PCBM molecules, respectively. The binding energy of the P3HT:PCBM layer with a LiF layer annealed for 3 min shifted to lower energy by as much as 0.3 eV in comparison with that of the P3HT:PCBM layer annealed for 5 or 10 min, indicating that the PCBM was dispersed around the P3HT, which had not high crystallinity. The S molecules were affected by the adjacent C molecules, for which the electronegativity was smaller, resulting in the low binding energy of the P3HT:PCBM layer annealed for 3 min. The surface crystallinity of the P3HT:PCBM layer was enhanced with increasing annealing time, which was confirmed by the XPS spectra. However, the XPS peak intensity of the S 2p peak decreased with increasing annealing time, indicative of a decrease in the amount of P3HT on the surface of the P3HT:PCBM layer.

The binding energy of the O 1s photoelectron peak of the P3HT:PCBM layer annealed for 3 min shifted to lower energy in comparison with that of the P3HT:PCBM layer with a LiF layer annealed for 5 or 10 min. The red shift of the O 1s peak for the P3HT:PCBM layer annealed for 3 min was attributed to the effect of the PCBM on the P3HT. The smaller shift of the O 1s photoelectron peak of the P3HT:PCBM layer annealed for 10 min

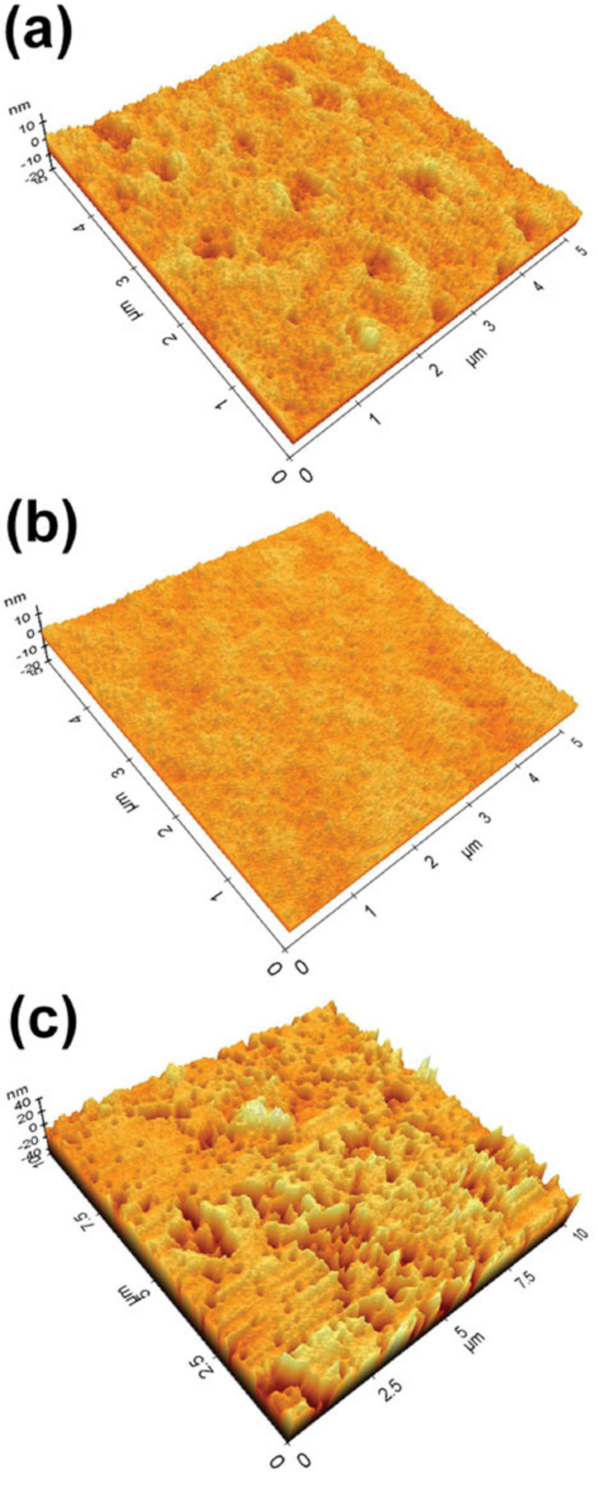

Figure 3. Atomic force microscopy images of the P3HT:PCBM layers with a LiF layer annealed for (a) 3, (b) 5, or (c) 10 min at 140°C.

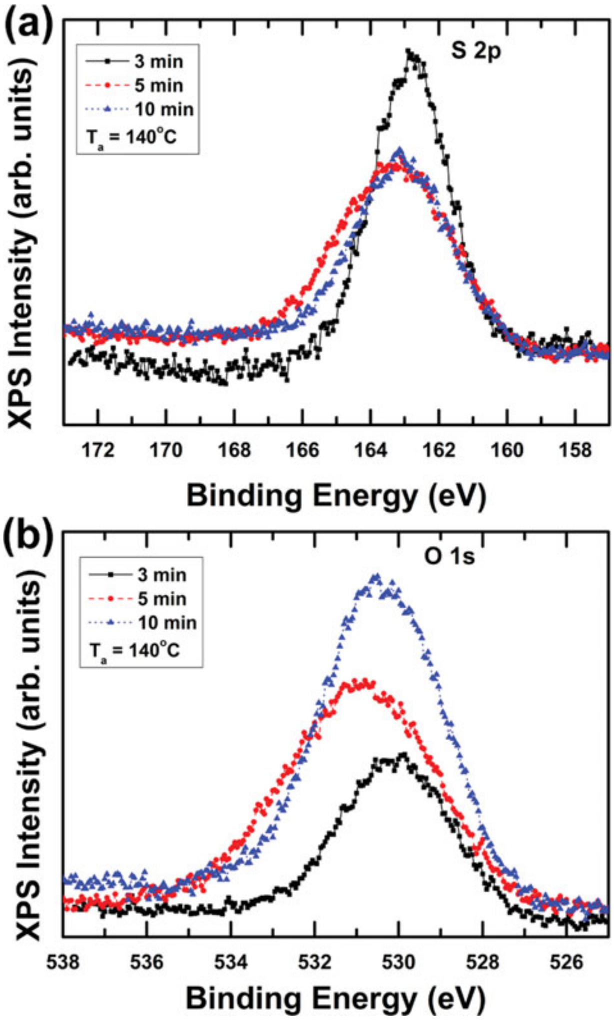

Figure 4. X-ray photoelectron spectroscopy spectra of the P3HT:PCBM layers with a LiF layer annealed for 3, 5, or 10 min at 140°C: (a) S 2*p* and (b) O 1*s* core levels.

in comparison with that of the P3HT:PCBM layer annealed for 5 min was related to the longer annealing time and resulted from the Li^+ ion diffusion into the active layer [15]. The diffusion of the Li^+ ions into the active layer resulted in an aggregation of the disturbed PCBM molecules. XPS results showed that the surface concentrations of the P3HT and the PCBM molecules decreased and increased with increasing annealing time. AFM images showed that the surface of the P3HT:PCBM layer with a LiF layer annealed for 10 min was rough due to the aggregation of the PCBM. The low absorption in the PCBM region for the P3HT:PCBM layer with a LiF layer annealed for 10 min originated from the aggregation of the PCBM molecules. Some parts of the surface for the PCBM/Al cathode caused non-uniform contacts between the Al cathode and the active layer and the generation of a dipole layer at the PCBM/Al heterointerface with the electric field from the Al to the PCBM, resulting in a decrease in V_{oc} [22].

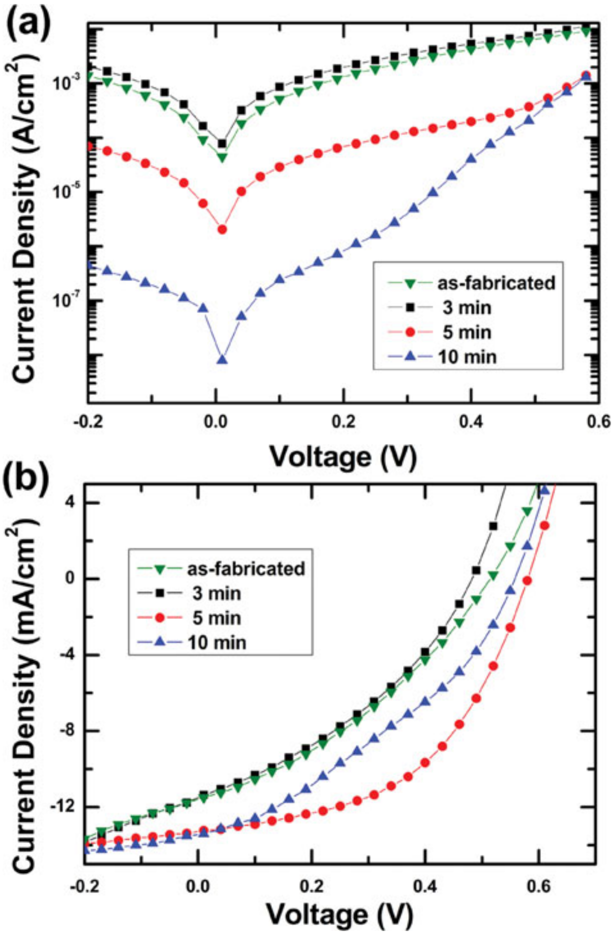

Figure 5. Current density-voltage curves of the as-fabricated photovoltaic cells based on the as fabricated P3HT:PCBM nanocomposites with a LiF layer and on those annealed for 3, 5, or 10 min at 140°C (a) in the dark and (b) under an AM 1.5 illumination power density of 100mW/cm^2.

Current-Voltage Measurement

Figure 5(a) shows the *J-V* curves of the as-fabricated OPV cells and of those annealed for 3, 5, or 10 min at 140°C. While the *J-V* curve of the as-fabricated device was similar to that of the device annealed for 3 min, the electrical performances of the devices annealed for 5 or 10 min were much better than that of the as-fabricated device.

Even though a 3-minute annealing time was not enough to affect the electrical properties of the device, a longer annealing time enhanced the device rectification. The leakage current of the annealed OPV cells decreased with increasing annealing time, indicative of good rectification. The OPV cells annealed for 10 min showed the best *J-V* curve. The enhancement of the annealed OPV cells was attributed to improved crystallinity of the active layer, resulting in a reduced leakage current. The *J-V* curves of the OPV cells annealed for 3, 5, or 10 min under a white-light illumination with a power density of 100 mW/cm^2 are shown in Fig. 5(b). Illumination with an A.M. 1.5 lamp with a power density

Table 1. Open-circuit voltage (V_{oc}), short-circuit current density (J_{sc}), fill factor (FF), and power conversion efficiency (PCE) of the as-grown photovoltaic cells and those annealed for 3, 5, or 10 min at 140°C under A.M. 1.5 illumination with power density of 100 mW/cm^2

Annealing time (min)	V_{oc} (V)	J_{sc} (mA/cm^2)	FF (%)	PCE (%)
3	0.482	11.50	36.1	2.01
5	0.581	13.28	50.1	3.87
10	0.558	13.45	35.0	2.64
as-fabricated	0.514	11.59	35.0	2.08

of 100 mW/cm^2 caused the Al/LiF/P3HT:PCBM/PEDOT:PSS/ITO device to function as a OPV cell. The V_{oc}, the short-circuit current density (J_{sc}), the fill factor (FF), and the PCE of the OPV cells are summarized in Table 1. The performance of the as-fabricated device was similar to that of the device annealed for 3 min. The V_{oc}, J_{sc}, and PCE of the OPV cells annealed for 3 min at 140°C are the lowest values among the annealed devices. The decrease in the V_{oc} for the device annealed for 3 min at 140°C was attributed to the high leakage current [23, 24], as shown in Fig. 5(a).

The active layers of the OPV cells annealed for 3 min at 140°C contained many defects, resulting in an increase in the leakage current. The J_{sc} of the OPV cells decreased due to the recombination between the defects in the active layer and photo-generated excitons [25]. When the OPV cells were annealed for 5 min at 140°C, their PCE was significantly improved. The values of the V_{oc}, J_{sc}, and PCE of the OPV cells annealed for 5 min at 140°C were 0.581 V, 13.28 mA/cm^2, and 3.87%, respectively. However, the PCE value of the OPV cells annealed for 10 min at 140°C decreased to 2.64%. While the J_{sc} value of the OPV cells annealed for 10 min was slightly higher than that of the devices annealed for 5 min, the corresponding V_{oc} and FF values were lower. Even though the OPV cells annealed at 10 min showed the lowest leakage current and the best rectification ratio, the PCE of the OPV cells annealed at 10 min was smaller than that of the devices annealed at 5 min. The degradation in the performance of the P3HT:PCBM layer annealed for 10 min was dominantly caused by a decrease in the light absorption, a non-uniform contact between the active layer and the Al cathode, and a decrease in the leakage current and rectification.

Conclusions

The effect of thermal annealing on the efficiency of heterojunction OPV cells fabricated utilizing P3HT and PCBM was investigated. Absorption spectra showed that the absorption intensity was the highest value for the P3HT:PCBM layer with a LiF layer annealed for 5 min, resulting in the enhancement of the PCE of the OPV cells. AFM images showed that the P3HT:PCBM layer annealed for 5 min had the smooth morphology among the several samples with various annealing times. The improvement of the surface morphology of the P3HT:PCBM layer annealed for 5 min was attributed to a high-quality heterointerface between the LiF layer and Al cathode, resulting in an effective decrease in the charge-transport distance and the contact resistance. The XPS peak intensity of the S 2p peak decreased with increasing annealing time, indicative of a decrease in the amount of P3HT on the surface of the P3HT:PCBM layer with LiF layer. The PCEs of the fabricated OPV cells annealed for 5 min was enhanced approximately 92% more than that of the OPV cells annealed for 3 or 10 min. These results can help improve understanding of the enhancement mechanisms of the PCE for the heterojunction OPV cells fabricated utilizing the P3HT:PCBM layer due to thermal treatment.

Funding

This research was supported by Basic Science Research Program through the National Research Foundation of Korea (NRF) funded by the Ministry of Education, Science and Technology (2013-016467).

References

[1] Morton, O. (2006). *Nature*, *443*, 19.

[2] Gadisa, A., Tvingstedt, K., Admassie, S., Lindell, L., Crispin, X., Andersson, M. R., Salaneck, W. R., & Inganas, O. (2006). *Synth. Met.*, *156*, 1102.

[3] Guo, Q., Kim, S. J., Kar, M., Shafarman, W. N., Birkmire, R. W., Stach, E. A., Agrawal. R., & Hillhouse, H. W. (2008). *Nano. Lett.*, *8*, 2982.

[4] Gupta, D., Mukhopadhyay, S., & Narayan, K. S. (2010). *Sol. Energy Mater. Sol. Cells*, *94*, 1309.

[5] Brabec, C. J., Cravino, A., Meissner, D., Sariciftci, N. S., Fromherz, T., Rispens, M. T., Sanchez, L., & Hummelen, J. C. (2001). *Adv. Funct. Mater.*, *11*, 374.

[6] Li, G., Shrotriya, V., Yao, Y., & Yang, Y. (2005). *J. Appl. Phys.*, *98*, 043704

[7] Servaites, J. D., Yeganeh, S., Marks, T. J., & Ratner, M. A. (2010). *Adv. Funct. Mater.*, *20*, 97.

[8] Peet, J., Kim, J. Y., Coates, N. E., Ma, W. L., Moses, D., Heeger, A. J., & Bazan, G. C. (2007). *Nat. Mater.*, *6*, 497.

[9] Green, M. A., Emery, K., Hishikawa, Y., Warta, W., & Dunlop, E. D. (2012). *Prog. Photovoltaics*, *20*, 12.

[10] Brabec, C. J., Shaheen, S. E., Winder, C., Sariciftci, N. S., & Denk, P. (2002). *Appl. Phys. Lett.*, *80*, 1288.

[11] Zhang, F., Ceder, M., & Inganas, O. (2007). *Adv. Mater.*, *19*, 1835.

[12] Kim, H. J., So, W. W., & Moon, S. J. (2007). *Sol. Energy Mater. Sol. Cells*, *91*, 581.

[13] Zhao, Y., Xie, Z., Qu, Y., Geng, Y., & Wang, L. (2008). *Synth. Met.*, *158*, 908.

[14] Ma, W., Yang, C., Gong, X., Lee, K., & Heeger, A. J. (2005). *Adv. Funct. Mater.*, *15*, 1617.

[15] Zeng, L., Tang, C. W., & Chen, S. H. (2010). *Appl. Phys. Lett.*, *97*, 053305.

[16] Karagiannidis, P. G., Kassavetis, S., Pitsalidis, C., & Logothetidis, S. (2011). *Thin Solid Films*, *519*, 4105.

[17] Dennler, G., Scharber, M. C., & Brabec, C. J. (2009). *Adv. Mater.*, *21*, 1323.

[18] Motaung, D. E., Malgas, G. F., Arendse, C. J., Mavundla, S. E., Oliphant, C. J., & Knoesen, D. (2009). *J. Mater. Sci.*, *44*, 3192.

[19] Kim, H. J., So, W. W., & Moon, S. J. (2006). *J. Korean Phys. Soc.*, *48*, 441.

[20] Huang, Y. C., Liao, Y. C., Li, S. S., Wu, M. C., Chen, C. W., & Su, W. F. (2009). *Sol. Energy Mater. Sol. Cells*, *93*, 888.

[21] Li, G., Shrotriya, V., Huang, J. S., Yao, Y., Moriarty, T., Emery, K., & Yang, Y. (2005). *Nat. Mater.*, *4*, 864.

[22] Song, Q. L., Li, C. M., Wang, M. L., Sun, X. Y., & Hou, X. Y. (2007). *Appl. Phys. Lett.*, *90*, 071109.

[23] Li, N., Lassiter, B. E., Lunt, R. R., Wei, G., & Forrest, S. R. (2009). *Appl. Phys. Lett.*, *94*, 023307.

[24] Chang, C. C., Lin, C. F., Chiou, J. M., Ho, T. H., Tai, Y., Lee, J. H., Chen, Y. F., Wang, J. K., Chen, L. C., & Chen, K. H. (2010). *Appl. Phys. Lett.*, *96*, 263506.

[25] Kim, M. S., Kim, B. G., & Kim, J. S. (2009). *ACS Appl. Mater. Interfaces*, *1*, 1264.